Electrochimica Acta 207 (2016) 143–151

Contents lists available at ScienceDirect

Electrochimica Acta

journal homepage: www.elsevier.com/locate/electacta

Electropolimerization of Functionalizaed Carbazole End-Capped Dendrimers. Formation of Conductive Films

María I. Mangione[a], Rolando A. Spanevello[a,*], Daniela Minudri[b], Daniel Heredia[b], Luciana Fernandez[b], Luis Otero[b], Fernando Fungo[b,*]

[a] Instituto de Química Rosario, Facultad de Ciencias Bioquímicas y Farmacéuticas, Universidad Nacional de Rosario – CONICET, Suipacha 531, S2002RLK Rosario, Argentina
[b] Departamento de Química, Universidad Nacional de Río Cuarto, Agencia Postal 3 (X5804BYA), Río Cuarto, Argentina

ARTICLE INFO

Article history:
Received 18 December 2015
Received in revised form 19 April 2016
Accepted 26 April 2016
Available online 28 April 2016

Keywords:
Dendrimeric Polymers
Electrodeposition
Optoelectronic

ABSTRACT

A series of peripherally carbazole functionalized dendrimeric starburst monomers were synthesized and characterized. The electrochemical polymerization over Pt and indium tin oxide electrodes of fully π-conjugated dendrimers allows the generation of electro-active polymeric films. Dendrimers were design with and without electroactive central core (triphenylamine) connected to peripherals moieties, which influence the physicochemical characteristics of the electrogenerated polymers. The versatile electropolymerization methodology allows the generation of thin films of hyperbranched macromolecules with good electrical conductivity, reversible electrochemical processes and electrochromic properties.

1. Introduction

Dendrimers are highly branched organic macromolecules formed by multiple chains emanating from a core, which hold a large number of applications in several fields [1–3]. In particular, for the use as components in organic electronic devices, these branches can be designed and synthetized as π-conjugated cables, to provide adequate charge transport capabilities [4–12]. In addition, functional groups such as chromophores, electron donor and/or electron acceptor moieties can be introduced in selected positions (dendrimers' core, branches or periphery), in order to obtain the desired electronic or optoelectronic characteristics. In this way, dendrimeric structures found numerous applications as light-harvesting antennas [13], organic light-emitting material [4–9], charge carriers transport layers [14], and as electron donor-acceptor material [7,10,12,15]. However, the preparation of functional dendrimers is usually a great challenge, since steric and solubility problems frequently appear during the syntheses stages. Steric hindrance could arise during the connection of dendrons to the focal point, and the solubility limitations often interfere in the production of high generation dendrimeric polymers. Thus, for the production of π-conjugated dendrimers it is important the search of alternative and efficient synthesis methods. During our research program about the development of organic materials for electronic and optoelectronic devices we demonstrated that hyperbranched π-conjugated polymeric materials can be formed electrochemically from suitable functional dendrimeric monomers [16–22]. The use of specially designed starburst dendrimer allows not only the polymer formation by electropolymerization, but also the deposition of the organic material over a conducting substrate as thin homogeneous films. In this last sense, we also proved that by controlling the condition of the electrochemical film formation, it is possible to optimize the film thickness and the surface morphology, with the consequent effects over the film optoelectronic properties [21].

In order to obtain the desired starburst dendrimeric monomers, the branched macromolecules must be carefully designed for to achieve the necessary electronic and optoelectronic properties. Dendrimeric materials with well-defined structures may be prepared by two main synthetic strategies, the convergent [23] and divergent [24] routes. In a convergent synthesis, the dendrimer is built from the periphery inward. This procedure gives rise to a precisely defined structure, monodisperse and with high purity by avoiding incomplete end groups. One of the drawbacks of convergent strategy is that it gives rise to a slow growth and, if high generation's dendrimers are needed, the convergent route could be a problem. In contrast, the divergent

* Corresponding authors.
E-mail addresses: spanevello@iquir-conicet.gov.ar (R.A. Spanevello), ffungo@exa.unrc.edu.ar (F. Fungo).

http://dx.doi.org/10.1016/j.electacta.2016.04.154
0013-4686/

route builds the dendrimer from the core outward. This route often offers more drawbacks than the convergent one. As the generation number increases, dendrimers' purity and polydispersity are more difficult to achieve, and restricts the repertory of reactions that could be applied to a few number of high yielding ones [23,24,25].

In this article, we report the synthesis and properties of peripherally carbazole (CBZ) functionalized starburst monomers, featuring the presence or absence of electroactive central core triphenylamine (TPA) moieties connected by conjugated or saturated branches (Fig. 1). The dendrimeric monomers are obtained by a convergent strategy. In addition, the CBZ residues allow the formation of hyperbranched polymeric films over conductive substrates by electrochemical polymerization. In fact, the radical cation coupling of oxidized CBZ drives into the growing of the dendrimeric structures. Two different fully π-conjugated dendrimeric polymers are formed, with and without electroactive central core connected to peripherals moieties (structures **1** and **3**, Fig. 1). Also, structurally related homologues dendrimeric monomers non-conjugated or without CBZ moieties (structures **4** and **2**) are studied, in order to establish physicochemical-properties/molecular structures relationships.

We showed that the new hyperbranched macromolecules obtained by the versatile electropolymerization methodology exhibit interesting electronic properties that yield thin films with good electrical conductivity, reversible electrochemical processes and stability. The outlined strategy allowed us to obtain new materials through a process simpler than flask synthesis, and provided one of the very few examples of using starburst monomers application to form electrochemically active polymers.

2. Materials and methods

2.1. Instrumentation and Characterization Techniques

Melting points were taken on a Leitz Wetzlar Microscope Heating Stage, Model 350 apparatus and are uncorrected. ^{1}H and ^{13}C NMR spectra were recorded on Bruker Avance-300 spectrometer with Me_4Si as the internal standard and chloroform-d as solvent. Abbreviations: s = singlet, d = doublet, t = triplet, and m = multiplet expected but not resolved. Mass spectra of dendrons were recorded in a Shimadzu QP2010 Plus instrument, ion source temperature = 300 °C, and detector voltage = 70 kV. Samples were analyzed by ultraviolet matrix assisted laser desorption-ionization mass spectrometry (UV−MALDIMS) and by ultraviolet laser desorption-ionization mass spectrometry (UV−LDI MS) performed on the Bruker Ultraflex Daltonics TOF/TOF mass spectrometer Mass spectra were acquired in linear positive and negative ion modes. Stock solutions of samples were prepared in chloroform. External mass calibration was made using β-cyclodextrin (MW 1134) with nHo as matrix in positive and negative ion mode. Sample solutions were spotted on a MTP 384 target plate polished steel from Bruker Daltonics (Leipzig, Germany). For UV−MALDI MS matrix solution was prepared by dissolving GA (gentisic acid, 1 mg/mL) in water and dry droplet sample preparation was used according to Nonami et al. [26] loading successively 0.5 μL of matrix solution, analyte solution and matrix solution after drying each layer at normal atmosphere and room temperature. For UV-LDI MS experiments two portions of analyte solution (0.5 μL × 2) were loaded on the probe and dried successively (two dry layers). Desorption/Ionization was obtained by using the frequency-tripled Nd:YAG laser (355-nm). The laser power was adjusted to obtain high signal-to-noise ratio (S/N) while ensuring minimal fragmentation of the parent ion sand each mass spectrum was generated by averaging 100 lasers pulses per spot. Spectra were obtained and analyzed with the programs FlexControl and FlexAnalysis, respectively. Reactions were monitored by TLC on 0.25 mm E. Merck Silica Gel Plates (60F254), using UV light (254 nm) and phosphomolybdic acid as developing agent. Flash column chromatographies using E. Merck silica gel 60H were performed by gradient elution of mixture of n-hexane and increasing volumes of dichloromethane or ethyl acetate. Reactions were run under an argon atmosphere with freshly anhydrous distilled solvents, unless otherwise noted. Yields refer to chromatographically and spectroscopically homogeneous materials, unless otherwise stated.

For the optical characterization a Shimadzu UV-2401PC spectrometer and a Spex FluoroMax fluorometer were used to measure the absorption and fluorescence spectra, respectively. Spectra were acquire using quartz cells (path length: 1 cm) at room temperature in 1,2-dichloroethane (DCE) and toluene (TOL) solutions.

The dendrimers electrochemical properties were studied in 0.5-1.0 mM range concentration in DCE electrolyte containing 0.1 M tetra-*n*-butylammonium hexafluorphosphate (TBAHFP) with an Autolab Electrochemical Instruments potentiostat. The voltammetric experiments were carry out using as working electrode an inlaid platinum disk (2.16×10^{-3} cm^2) polished on a felt pad with 0.3 μm alumina and sequentially sonicated in water and absolute ethanol, silver wire as pseudo-reference electrode and a platinum coil as the counter electrode. Before each experiment electrolyte blank was made to discard possible electrochemically active interferes. All potential values reported are expressed relative to ferrocene/ferrocenium redox couple (Fc/Fc^+ = 0.40 V vs SCE), which was used as an internal standard [27].

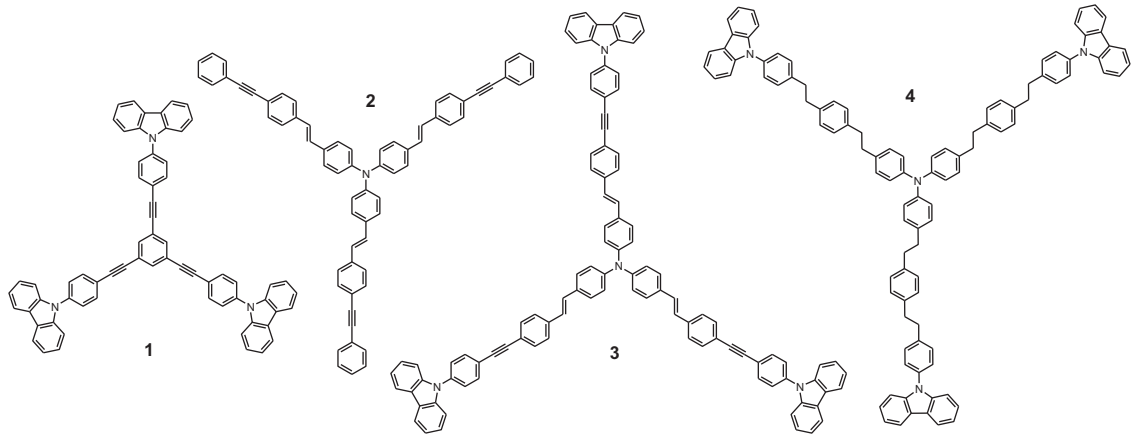

Fig. 1. Dendrimer structures.

The spectroelectrochemical experiments were carried out in a homemade cell built from a commercial UV-visible cuvette. The films were obtained by electropolimerized on ITO (indium tin oxide, Delta Technologies, nominal resistance 10 Ω/square) electrodes by cyclic voltammetry technique under the experimental conditions described above. The coated ITO- polymer film was used as working electrode, Pt as counter electrode and a silver wire was used as pseudo-reference electrode. The homemade cell was placed in the optical path of the sample light beam Hewlett Packard 8453 diode array spectrophotometer, and UV-visible light absorption spectra were taken under potential control. The background correction was obtained by taking an UV-visible spectrum of an ITO working electrode without the polymer film. Surface analysis of electrodeposited polymer films on ITO electrodes was performed by scanning electron microscopy (SEM) with a Carl Zeiss EVO MA 10 with electron beam energy of 18 KV.

2.2. Synthetic Procedures

2.2.1. Dendrimer **1**

Dendron **9** (470.6 mg, 1.28 mmole) was dissolved in anhydrous toluene (10 mL) under argon atmosphere. $Pd(PPh_3)Cl_2$ (11.6 mg, 0.02 mmole), CuI (6.1 mg, 0.03 mmole) and PPh_3 (6.7 mg, 0.03 mmole) were added and the mixture was stirred for 30 minutes at room temperature. After the solution became orange, anhydrous trimethylamine (10 mL) was added and the reaction was stirred for additional 15 minutes. Triethynylbenzene **7** (48.0 mg, 0.32 mmole) was added and the mixture was stirred 48 hs at 76 °C. The solvents were concentrated under vacuum and the crude product was purified by flash chromatography (hexane: dichloromethane) yielding dendrimer **1** as white solid (257.2 mg, 0.29 mmole). mp: 297– 299 °C (dichloromethane:hexane); ^{1}H NMR: ≏ (300 MHz, $CDCl_3$, TMS): 8.15 (d, J = 7.59 Hz, 6H), 7.84–7.73 (m, 6H), 7.70–7.54 (m, 8H), 7.51–7.36 (m, 13H), 7.31 (dd, J = 6.36 Hz, 6H); ^{13}C NMR: ≏ (75 MHz, $CDCl_3$, TMS): 140.52, 138.06, 135.36, 133.28, 126.94, 126.13, 124.07, 123.65, 121.66, 120.44, 120.34, 109.77, 90.08, 88.66. MALDI-TOF MS: calcd for $C_{66}H_{39}N_3$, (MH^+) m/e 875., m/e 875.2 (MH^+).

2.2.2. Dendrimer **2**

To a mixture of **6** (64.8 mg, 0.07 mmol) in dry toluene were added triethylamine 1:1 (14 mL) $Pd(PPh_3)_4$ (11.4 mg, 0.01 mmol), CuI (2.4 mg, 0.01 mmol), and triphenylphosphine (2.5 mg, 0.01 mmol), and the mixture was stirred 15 min under argon atmosphere. Commercial phenylacetylene **13** (0.05 mL, 0.43 mmol) was added and the reaction was stirred overnigthat 80 °C. The solvent was evaporated and the crude product was purified by column chromatography yielding 51.7 mg (0.06 mmol, 87%) of dendrimer **2** as yellow solid. mp: 122– 125 °C. ^{1}H NMR, δ (300 MHz, $CDCl_3$, TMS): 7.56–7.52 (m, 7H), 7.50 (d, J = 4.6 Hz, 9H), 7.47–7.40 (m, 8H), 7.38–7.32 (m, 9H), 7.16–7.07 (m, 9H), 7.01 (d, J = 16.3 Hz, 3H). ^{13}C NMR, δ (75 MHz, $CDCl_3$, TMS): 146.81, 137.48, 132.06, 131.95, 131.60, 128.90, 128.37, 128.25. 127.63, 126.75, 126.26, 124.31, 123.34, 122.00, 90.28, 89.64. MALDI–TOF (m/e): calcd for $C_{90}H_{63}N_3$, 1186.5 (MH +); obsd, 1186.4 (MH +).

2.2.3. Dendrimer **3**

Core **6** (44.0 mg, 0.05 mmole) was dissolved in anhydrous toluene (7.0 mL) under argon atmosphere. $Pd(PPh_3)_4$ (5.4 mg, 0.005 mmole) and CuI (1.6 mg, 0.008 mmole) were added and the solution was stirred 30 minutes at room temperature. Then, anhydrous trimethylamine (5 mL) was added and the yellow mixture was stirred for additional 15 minutes. Dendron **12** (56.8 mg, 0.22 mmole) was added and the reaction was stirred and heated to reflux during 48 hs. At the end, the mixture became orange. Solvents were concentrated under vacuum and the crude product was purified by flash chromatography (hexane:dichloromethane) affording dendrimer **2** (52.2 mg, 0.039 mmole, 82%) as orange solid. mp: 183 – 186 °C (dichloromethane:hexane); ^{1}H NMR: ≏ (300 MHz, $CDCl_3$, TMS): 8.16 (d, J = 7.65 Hz, 6H), 7.77 (d, J = 8.25 Hz, 6H), 7.61–7.50 (m, 18H), 7.49–7.42 (m, 17H), 7.35–7.27 (m, 7H), 7.19–7.10 (m, 9H), 7.04 (d, J = 16.48 Hz, 3H); ^{13}C NMR: ≏ (75 MHz, $CDCl_3$, TMS): 146.85, 140.57, 137.74, 137.55, 135.23, 133.09, 132.05, 130.25, 129.08, 127.68, 126.87, 126.35, 126.08, 124.34, 123.58, 122.32, 121.74, 120.40, 120.24, 109.77, 90.63, 89.61. MALDI-TOF MS: m/e 1346.4 (M^+).

2.2.4. Dendrimer ***4***

Dendrimer **3** (38.0 mg, 0.028 mmole) was dissolved in distilled THF (9.0 mL) at room temperature affording a bright green solution. Catalyst Pd/C 10% (23.3 mg) was added and the mixture was submitted under hydrogen pressure (9 atmospheres) for 3 days. After this reaction time, green color of the suspension remained and more Pd/C 10% (29.0 mg) was added and the reaction was stirred under 9 atmospheres for 2 additional days. Finally, the reaction mixture showed no fluorescence and was filtered over a short pad of Celite, washing with dichloromethane. Solvents were concentrated under reduce pressure and the crude product was purified by flash chromatography (hexane:dichloromethane) to afford dendrimer **4** (33.6 mg, 0.024 mmole, 86%) as colorless oil. ^{1}H NMR: d (300 MHz, $CDCl_3$, TMS): 8.15 (d, J 7.7 Hz, 6H), 7.47 (d, J 8.4 Hz, 6H), 7.44–7.36 (m, 18H), 7.33–7.26 (m, 6H), 7.17 (s, 12H), 7.07 (d, J 8.6 Hz, 6H), 7.00 (d, J 8.5 Hz, 6H), 3.03 (s, 12H), 2.90 (s, 12H). ^{13}C NMR: d (75 MHz, $CDCl_3$, TMS): 37.41, 37.47, 37.60, 37.70, 109.79, 119.76, 120.27, 123.26, 123.87, 125.85, 127.02, 128.45, 128.51, 129.11, 129.86, 135.46, 135.94, 139.03, 139.66, 141.01, 141.26, 146.01.

3. Results and discussion

3.1. Synthesis and Characterization

All dendrimers (Fig. 1) were obtained by Sonogashira coupling between the cores 1,3,5-triethynylbenzene (TEB) **5** or tris{4-[(E)-2-(4-iodophenyl)vinyl]phenyl}amine **6** and the corresponding dendrons by exception of dendrimer **4** which was obtained by hydrogenation of dendrimer **3**. The synthesis of cores **5** and **6** were previously described by our group (Fig. 2) [22].

Synthesis of phenyl carbazole dendrons **9** and **12** were accomplished starting from commercial carbazole **7**. Under modified Ullmann's conditions **7** was coupled with 1,4-diiodobenzene **8** to afford **9** in 76% yield. Sonogashira type coupling reaction of **9** with commercially available reagent **10** generates protected alkyne **11** with 97% of yield. Finally, **11** was deprotected under basic conditions to produce free alkyne **12** in 86% of yield. All the compounds were purified by flash column chromatography and all the synthetic steps gave very good yields (Scheme 1).

Dendrimers were obtained by coupling between core **5** and dendron **9** and core **6** with dendron **12** and commercial

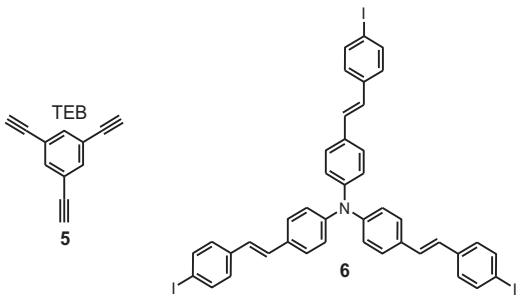

Fig. 2. Cores 5 (TEB) and 6.

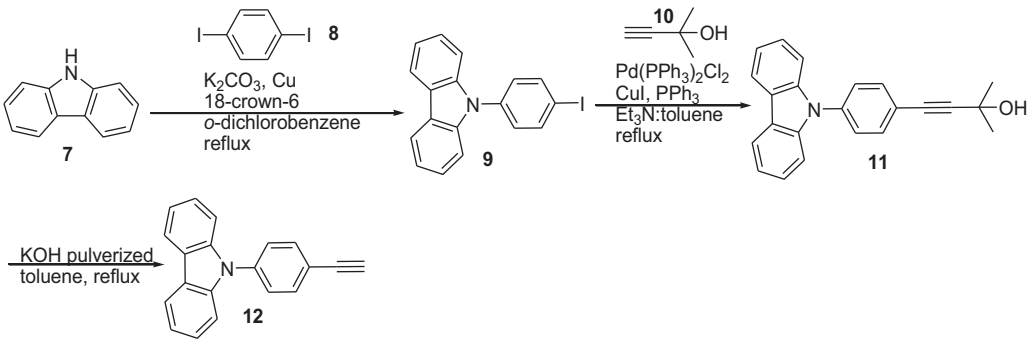

Scheme 1. Synthesis of dendrons 9 and 12.

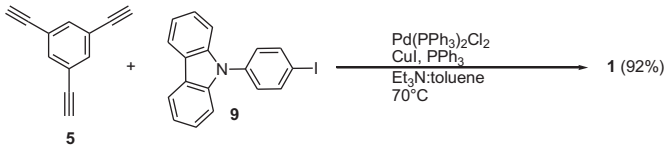

Scheme 2. Synthesis of dendrimer 1.

phenylacetylene **13**. Palladium catalyst $Pd(PPh_3)_2Cl_2$ catalyst was employed for the coupling reactions of core **5** with dendron **9** (Schemes 2 and 3).

$Pd(PPh_3)_4$ was an efficient catalyst when performing the cross-coupling reaction between core **6** and dendrons **12** and **13**. As depicted in Scheme 3 reactions yields were good to very good. All dendrimers were purified by flash chromatography and recrystallized producing white to orange solids for the compounds with extended π-conjugation. Dendrimer **4** was prepared by catalytic hydrogenation of **3** under 9 atmosphere of hydrogen pressure using Pd/C as catalyst and distillated tetrahydrofuran as solvent. Product **4** was obtained as colorless oil in 86% yield.

The cores and dendrons structures were confirmed by ^{1}HNMR, ^{13}CNMR and FTIR spectroscopy, and compared with the corresponding bibliographic reference when it is necessary. Structures of the dendrimers were also characterized by ^{1}HNMR, ^{13}CNMR, FTIR spectroscopy and MALDI-TOF mass spectrometry experiments. In the conjugated macromolecules **1**, **2** and **3** the observation of two alkyne signals and the total number of different carbon atoms signals in the ^{13}CNMR spectrum allowed us to confirmed the "starburst" shape of the dendrimers. Dendrimer **4** showed no alkyne signals in ^{13}CNMR spectrum and four new methylene peaks were observed. In the ^{1}HNMR spectrum broad signals at 2.90 and 3.03 ppm corresponding to a total of 24 protons demonstrated the completed hydrogenation of all the unsaturated bonds present in the starting macromolecule **3**. MALDI-TOF data confirmed the expected molecular mass calculated for each dendrimer. Experimental details and NMR spectra are described in the Supporting Information.

3.2. Starburst Dendrimeric Monomers Optical Properties

The dendrimers electronic transitions were investigated by measuring their absorption and fluorescence spectra in diluted solutions. Fig. 3 shows the absorption and photoluminescence spectra in DCE and TOL solutions.

The monomers light absorption energies are nearly solvent polarity independent, and exhibit similar profiles. In general, the optical behavior can be analyzed and understood by taking into account the different chromospheres that composed the molecular structures (CBZ, TPA and *para*-phenylenevinylene). Dendrimer **1** is constituted by three CBZ moieties bonded through ethynylphenyl arms linked to the *meta*-positions of the central phenyl ring. In its spectrum the three main transitions (See Fig. 3**a** and Table 1) are characteristic of those found in 9-phenylcarbazole derivatives compounds [28–32]. On the other hand, dendrimer **3** presents four identifiable optical transitions with λ_{max} at 238, 293, 342 and 418 nm (See Fig. 3**b** and Table 1). The low energy band (not present in **1**) can be attributed to the π–π^* transition taking place in the *para*-phenylenevinylene segment [22]. This band assignment is supported by the comparison with the spectrum of the model dendrimer **2**, which holds three vinylene-modified phenyls linked to a TPA core (See Fig. 3**c**). Following this analysis, the absorption spectrum of dendrimer **3** can be seen as a combination of those obtained with molecular structures of dendrimers **2** and **1**. In fact, the dendrimer core is the same in molecules **3** and **2** and the external shell resembles to dendrimer **1**. In comparison, when the conjugated arms of dendrimer **3** are hydrogenated to produce

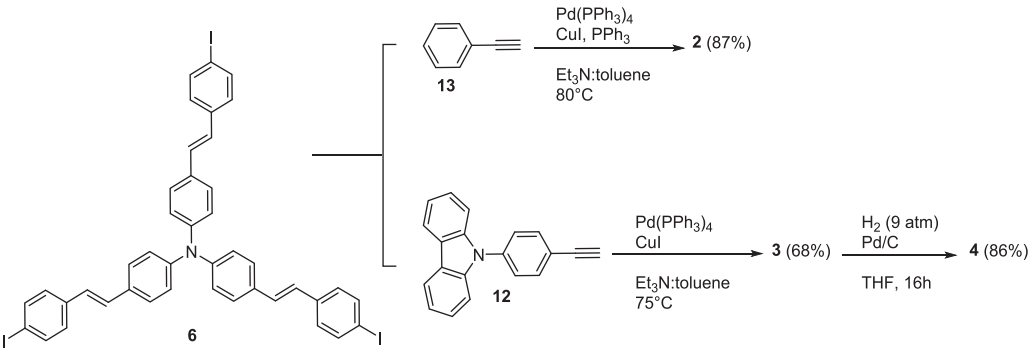

Scheme 3. Synthesis of dendrimers 2, 3 and 4.

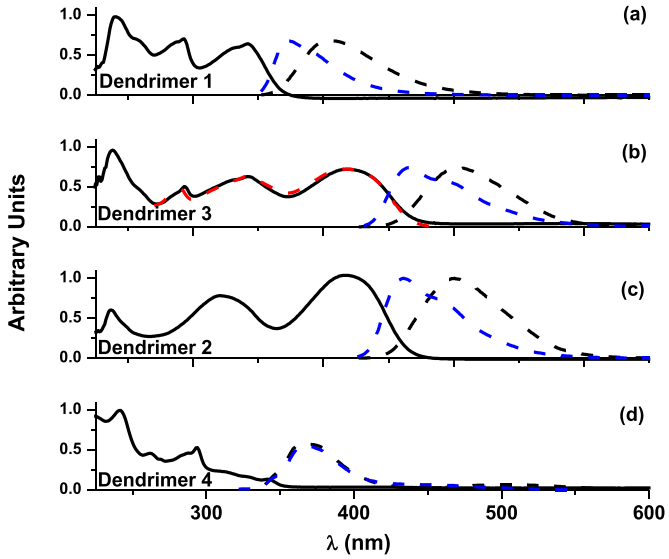

Fig. 3. Normalized absorption (—) and emission (- - -) spectra of a) Dendrimer 1, b) Dendrimer 3, c) Dendrimer 2 and d) Dendrimer 4 recorded in DCM (black) and TOL (Blue). Since the dyes spectra are similar in DCM and TOL, only the light absorption spectra in DCM are shown. In Fig. 3b the dendrimer 3 photoluminescent excitation spectrum (measured at 505 nm in DCE) is showed with red dash line (- - -). (For interpretation of the references to colour in this figure legend, the reader is referred to the web version of this article.)

compound **4**, the obtained electronic absorption spectrum lacks of the optical transition attributed to the vinylene residues (See Fig. 3**d**).

The photoluminescence properties of dendrimers were studied in DCE and TOL solution exciting the monomers at the wavelength maxima of the lower energy bands. The obtained results are showed in Fig. 3 and summarized in Table 1. It is possible to see that the dendrimers that hold *para*-vinylene moiety (dendrimers **2** and **3**) prevail the emission of this well known light emitting center, while hydrogenated dendrimer **4** shows blue emission typical of TPA and CBZ centers [22,31–33]. In the case of dendrimer **1** that holds in its structure ethynylphenyl moiety, the emission from CBZ center is red shifted regarding unsubstitute carbazole in 9 position, due to the larger conjugation extension [32]. In addition, from the analysis of the showed fluorescence spectra, it can be observed differences between the dendrimers emission with the changes in the solvent polarity. Analyzing Fig. 3 it could be observed that dendrimers **2** and **3** shown approximately 35 nm bathochromic shifts in their emission maxima when the solvent polarity is increased from TOL to DCE. This effect is in agreement with a decrease in the energy of the singlet excited states as a function of an increase in the solvent polarity; originated from fluorophores that have larger dipole moments in the excited state than in the ground state [22,32,34]. Similar solvent effect is observed in dendrimer **1** fluorescence emission spectra. However, the fluorescence of dendrimer **4** is almost insensitive to the solvent polarity. Thus, the extension of the conjugation through the introduction of unsaturated multiple bonds confers to the dendrimers excited states a higher polar character [32]. Furthermore, as it is shown in Fig. 3**b**, dendrimer **3** photoluminescent excitation spectrum measured at 505 nm in DCE solution (dashed red line in Fig. 3**b**), presents similar spectral features as their corresponding absorption spectrum. This observation is indicative that the nitrogenated chromospheres (CBZ) efficiently contribute to the *para*-phenylenevinylene emission at 505 nm, proving the existence of intramolecular energy transfer in dendrimer **3** branches [22,32,35].

Table 1
Photophysical and electrochemical parameters of 1–4 dendrimers. The emission spectra were measured by excitation at the maximum of the lower energy bands in nm. [a] Irreversible peak. [b] Half-wave potentials, obtained from reference [22].[c] Reversible process. [d] Onset potentials determined from intersection between the baseline and the current signal. The potentials values are expressed in volt vs. Fc/Fc^+.

DENDRIMER	PHOTOPHYSICAL			ELECTROCHEMICAL	
	Absorption($\lambda_{máx}$)	*Emission*($\lambda_{máx}$)		*Oxidation Potentials (V)*	
	DCE	DCE	TOL	$E_{Monomer}$	E_{Film}
Dendrimer 1	241/293/342	406	373	0.95[a]	0.41[d]
Dendrimer 2	321/419	501	462	0.38[b]	——
Dendrimer 3	238/293/342/418	505	466	0.37[c]/0.98[a]	0.44[d]
Dendrimer 4	243/261/294	365	366	0.36[c]/0.82[a]	0.40[d]

3.3. Dendrimers Electrochemical Properties: Electropolymerization and Film Formation

The electropolymerization of fully conjugated dendrimers (dendrimers **1** and **3**) allows the generation of hyperbranched macromolecules obtained as thin films over both, Pt and ITO electrode surfaces, with good electrical conductivity and electrochemical stability. The dendrimers electrochemical behavior and the radical ions stability were studied by cyclic voltametry technique in DCE solution. Compound **1**, as it has been mentioned, possesses CBZ as unique electroactive center in their outer layer. Therefore, it is expected that this moiety rules the dendrimers electrochemical behavior. Fig. 4**a** shows the cyclic voltammograms of **1**. It can be observed that in the first scan from −0.25 V to positive potentials (blue line) an oxidation wave, with peak at 0.95 V, is generated (Table 1). When the scan direction is inverted two reduction waves can be detected; one at 0.86 V (complementary to the process at 0.95 V) and another at 0.56 V. During the second cycle (red line) a new oxidation peak at 0.67 V is identified, which is complementary to the reduction process at 0.56 V observed in the first cathodic sweep. This electrochemical behavior is typical of carbazole derivates where the CBZ oxidation leads to the formation of radical cations, which undergoes a dimerization reaction to produce dicarbazole [17,18,20,33,36]. The obtained dimer is more conjugated, thus it is more easily oxidizable than the starting monomers, producing a new voltamperometric signal at 0.67 V. As dendrimer **1** holds in its molecular structure three CBZ residues, it is possible the electrochemical generation of hyperbranched dendrimeric polymers which are deposited as a

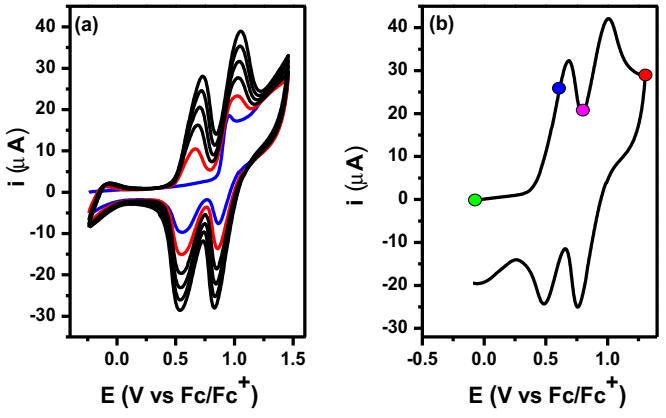

Fig. 4. a) First (blue) and second (red) cycles in repetitive voltammograms (black) of dendrimer 1 solution (DCE, 0.1 M TBAHFP) on a Pt electrode, v = 0.1 V s^{-1}. b) Cyclic voltammogram of the electro-deposited film derived from dendrimer 1 on Pt (DCE, 0.1 M TBAHFP). The superimposed colored dots on voltammogram trace correspond to the potentials applied when the spectra showed in Fig. 7a were acquire. (For interpretation of the references to colour in this figure legend, the reader is referred to the web version of this article.)

conducting film [17,18,20,36]. This hypothesis is corroborated when the electrode potential is continually cycled. The progressive growth of the peaks current (Fig. 4**a,** black lines) denoted the development of a conducting and electroactive film on the working electrode surface. Further confirmation can be reach when the electrode is removed from the electrochemical cell, washed with solvent, and transferred to free monomer supporting electrolyte solution. The redox response of this modified electrode is shown in Fig. 4**b**. It can be observed two oxidation peaks at 0.68 V (onset potential 0.41 V, Table 1) and 1.01 V, and two cathodic waves at 0.49 and 0.77 V. Thus, the CBZ moieties oxidation process in **1** results in dimerization reactions, which leads to the formation of a stable polymer on the electrode surface [17,18,20,36]. In concordance, spectroelectrochemical studies also supported this conclusion (see below).

Dendrimer **3** has peripheral CBZ groups like compound **1** but the core of the dendrimeric structure holds a TPA residue, which resembles dendrimer **2** (see Fig. 1). In Fig. 5**a** (blue line voltamogram) can be observed a first reversible wave at 0.37 V, and a second oxidation process at 0.98 V. When the potential scan is inverted to cathodic direction it is observed a main peak, centered around 0.55 V. Taking into account that the CBZ groups have a higher oxidation potential than TPA unit [17,20,22,33,36], it is possible to assign the first electrochemical process to the dendrimer core (TPA), and the second anodic peak to the outer sphere residues (CBZ groups) oxidation. Moreover, when the applied potential is swept until the first redox process, a reversible electrochemical response is clearly observed (See inset in Fig. 5**a**), similar than those obtained for dendrimer **2** [22]. In concordance, if the potential is successively cycled until this first wave, a current growth associated with the electrodeposition of a conducting film at the electrode surface is not detected. This is in agreement with the tri-*para*-substituted TPA radical cation stability [17,20,22].

On the other hand, when the applied potential is driven until the second redox process (assigned to the CBZ moieties oxidation), the dendrimer **3** starts an oxidative polymerization, generating a hyperbranched electroactive structure. Thus, through potentiodynamic cycles, a gradual increase of current is detected, indicating the formation of a conducting film on the electrode surface (see Fig. 5**a**). In order to study the redox behavior of the electrogenerated film, the working electrode was removed from the electrochemical cell and washed with DCE to eliminate the monomer that could remain on the electrode. Then, it was transferred to an electrolyte solution to study the modified electrode electrochemistry. The obtained voltamogram showed in Fig. 5**b** confirms that an electroactive film is irreversibly adhered to the electrode surface. The film has two reversible oxidation processes with peaks potential at 0.72 V (potential onset 0.44 V, Table 1) and 0.98 V, respectively. The polymeric film shows great stability when the film is subjected to numerous oxidation-reduction cycles. This behavior is similar to the one observed in other systems formed by electroactive polymers derived from CBZ [17,20,22,33].

Fig. 6 shows the hydrogenated dendrimer **4** voltammetric response, which has a non-conjugated structure between the CBZ peripheral groups and the TPA core (see Fig. 1). The obtained waves are quite similar to those generated by parent dendrimer **3**, with two main oxidation processes at 0.36 V and 0.82 V (Table 1). As before, these peaks can be assigned to the oxidation of TPA and CBZ centers, respectively. When the electrode applied potential is cycled until the first oxidation wave, a reversible redox process is generated, as can be observed in the black line voltammogram showed as inset in Fig. 6**a**. In the same inset is also shown with blue line the complete potential sweep until the second redox wave, where is possible to see the carbazole dimerization process, as was already described. Consequently, if the potential scan is repetitively cycled until the further oxidation peak, it is observed the characteristic growth and deposition of an electroactive film. The electrochemical response of dendrimer **4** film is shown in Fig. 6**b**, where two defined peaks are detected at 0.57 and 0.98 V, with a film oxidation potential onset of 0.40 V (Table 1).

A comparative analysis of the electropolymerization processes between dendrimer **4** with **1** and **3** (**Fig.s 4a, 5a** and **6a**), allows to observe that in the former case the current increase between successive voltammetric cycles is significantly lower than the one for fully conjugated dendrimers. This effect is a clear indication that, under the present experimental conditions, **4** is able to generated CBZ coupling, but the film formation efficiency is much lower compare with others dendrimers structures. In the case of dendrimer **4**, it is necessary to applied nearly hundred of voltammetric cycles on Pt electrode, to obtain a film with similar current characteristic than those generated after five voltammetric cycles with dendrimer **1** and **3**. This behavior has been already observed in other structural related non-conjugated dendrimers, and has been attributed to the higher solubility of the electro-oxidation products, that avoids the necessary electrode surface-

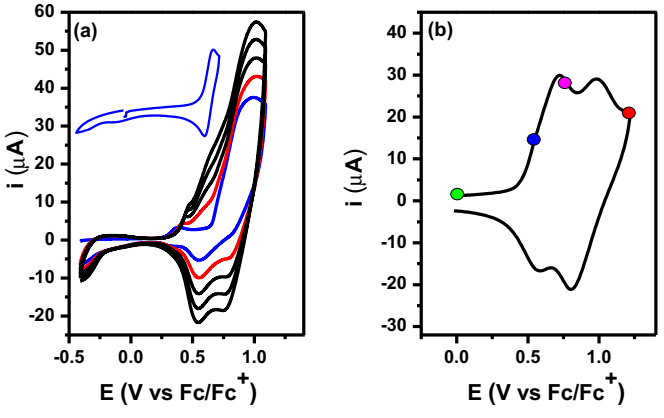

Fig. 5. a) First (blue) and second (red) cycles in repetitive voltammograms (black) of dendrimer 3 solution (DCE, 0.1 M TBAHFP) on a Pt electrode, v = 0.1 Vs^{-1}. Inset shows the cyclic voltammogram until the first oxidation wave. b) Cyclic voltammogram of the electro-deposited film derived from dendrimer 3 on Pt (DCE, 0.1 M TBAHFP). The superimposed colored dots on voltammogram trace correspond to the potentials applied when the spectra showed in Fig. 7b were acquire. (For interpretation of the references to colour in this figure legend, the reader is referred to the web version of this article.)

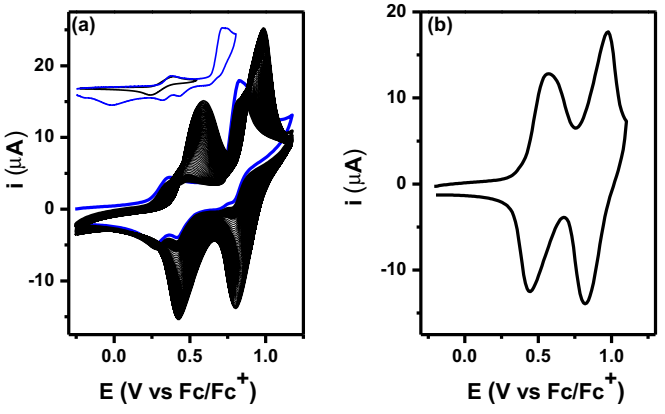

Fig. 6. a) First (blue) cycles of repetitive cyclic voltammograms of a solution of dendrimer 4 in DCE with 0.1 M of TBAHPP on a Pt at a scan rate of v = 0.1 Vs^{-1}. Inset shows in black line the cyclic voltammogram until the first oxidation wave. b) Cyclic voltammogram of the electro-deposited film derived from dendrimer 4 on Pt in DCE solution without monomer, v = 0.1 Vs^{-1}. (For interpretation of the references to colour in this figure legend, the reader is referred to the web version of this article.)

organic molecule interaction necessary for the film formation [22]. The higher solubility of dimers and/or oligomers originated by the coupling of **4** radical cations can be related to the rotational and conformational freedom degrees in the dendrimers arms that allow the generation of globular shape products, which do not remain on the electrode surface. Moreover, due to the low tendency of **4** to form electrodeposited films, it was not possible to modified ITO electrodes; precluding the possibility of studying its spectroelectrochemical properties (see below). These results reinforce the fact that the presence of conjugate and rigid branches in the dendron molecular structure is an important factor to obtain hyperbranched electropolymeric films [22].

3.4. Spectrolectrochemical Properties of Electrodeposited Films

The spectrochemical experiments on hyperbranched polymers electrodeposited as films over ITO electrodes were carried out in order to get information about the polymeric structures, and its relationship with the optoelectronical properties of the new materials. The films over semitransparent ITO electrodes were growth using the same experimental conditions already described for Pt electrode. The electronic absorption spectra at different applied potentials for dendrimer **1** are shown in Fig. 7**a**. The film derivate from **1** in its neutral state is almost transparent in the visible region. It has one defined absorption peaks at 346 nm, while that at higher energy wavelength the ITO light absorption onset does not allow the data acquisition. When the applied potential is moved to positive values, and reaches the first oxidation wave onset (0.41 V, Table 1), new electronic transitions are evidenced as new bands; one with wavelength absorption maxima at about 433 nm and a second broad band centered at 1016 nm. Also in Fig. 7**a** can be observed how these bands become well defined peaks as the potential advances through the first oxidation processes of dendrimer **1** film (see colored dots in Fig. 5**b**). These bands can be assigned to the generation of bicarbazole radical cations formed by oxidation of the polymeric film As the potential goes insides in the seconds oxidation process, the former absorption bands starts to decrease in absorbance, while a new broad band at 775 nm is develop, which is due to the light absorption by biscarbazole dication species [17,20,36,21].

On the other hand, a suitable film of dendrimer **3** was grown over an ITO electrode by cycling the potential in the conditions showed in Fig. 5**b**, in order to develop spectroelectrochemical analysis. At 0 V (green line, Fig. 7**b**), the film exhibited two identifiable light absorption waves at 335 and 657 nm (with a shoulder at 548 nm). The band at 657 nm is not observed in polymer **1** spectroelectrochemical analysis (see Fig. 5**a**), and consequently, it must be attributed to the presence of TPA group in dendrimer **3** polymeric film. This last band can be assigned to the typical electronic transition in TPA radical cations [22,36,37], which indicates that in the film generated from **3**, positive charges remain trapped or isolated in the dendrimer core, even at low potential. As it was observed with **1**, when the applied potential became more anodic, first the biscarbazole radical cation optical signals start to growth at 437 nm and ~1034 nm (see Fig. 5**a** and **b**), and then the biscarbazole dication is generated which exhibits a broad absorption band centered at 722 nm [22,36,37] Thus, the spectroelectrochemical analysis is in agreement with the electrochemical processes associated to the TPA central core and peripheral CBZ units in hyperbranched polymeric structure.

Therefore, the described spectroelectrochemical behavior supports that CBZ-CBZ electroactive centers is present as cross-linked in the molecular structure of dendrimeric films. A proposed molecular structure is shown in Fig. 8, where the dimerizations of CBZ moieties are involved in the electropolymerization processes of both monomers.

On the other hand, the UV–vis absorption changes with the applied potentials observed in dendrimeric films are fully reversible and associated with significant color changes that can be appreciate by the naked eye. Fig. 9**a** shows photographic pictures of a dendrimer **1** film in its neutral (applied potential, E_{app} = 0.00 V), semioxidized (E_{app} = 0.60 V), and fully oxidized (E_{app} = 1.25 V) states.

The film colorations (transparent, pale yellow, and green, respectively) exhibit a homogenous spreading on the ITO surface, showing the electrochromic capability of the material. Fig. 9**b** displays the sequential changes in transmittance at 772 nm when the applied potential is step-switched between the neutral and oxidized states (E_{app} 0.00 and 1.25 V). As can be seen, dendrimer **1** film possess a high contrast ratio, with transmittances of around 90 and 10% in the neutral and fully oxidized states, respectively. Furthermore, Fig. 9**c** exhibit the current changes associate to the coloration processes. These changes reflect the kinetics of the charge transport processes, and can be correlated with the coloration response time. The elapsed time needed for 90% of full transmittance changes at 772 nm were 7.0 s for the coloration step and 2.0 s for the bleaching step, reflecting the different conductivities between the reduced and oxidized forms of dendrimer **1** film. On the other hand, similar elecrochromic behavior was obtained with **3** electropolymer. However, the

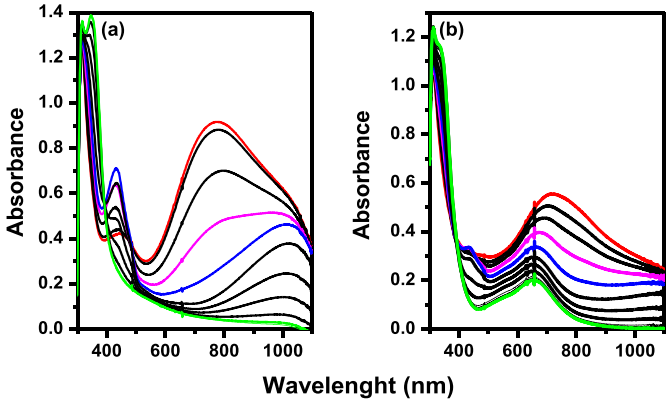

Fig. 7. UV-visible absorption spectra of electrodeposited films on an ITO electrode as function of applied potentials: a) dendrimer 1 and b) dendrimer 3. The potential applied to the colored spectra corresponds to the superimposed dots on voltammogram trace showed in Fig. 4b and 5 b with the same color. The insets show pictures of the electrodes at different redox states.

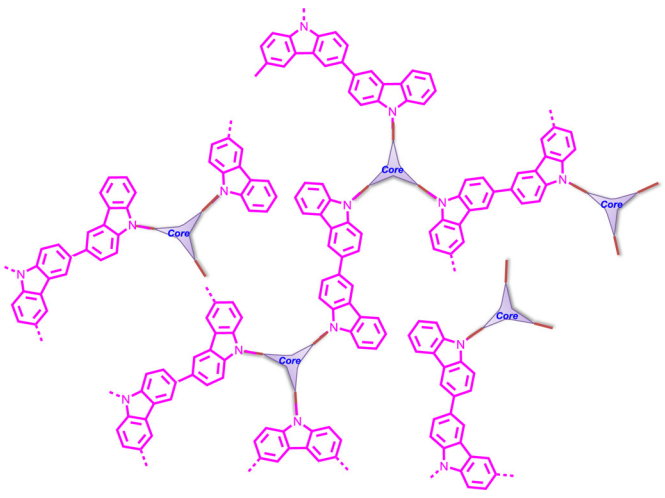

Fig. 8. Electrochemical polymerization of end-capped CBZ dendrimers.

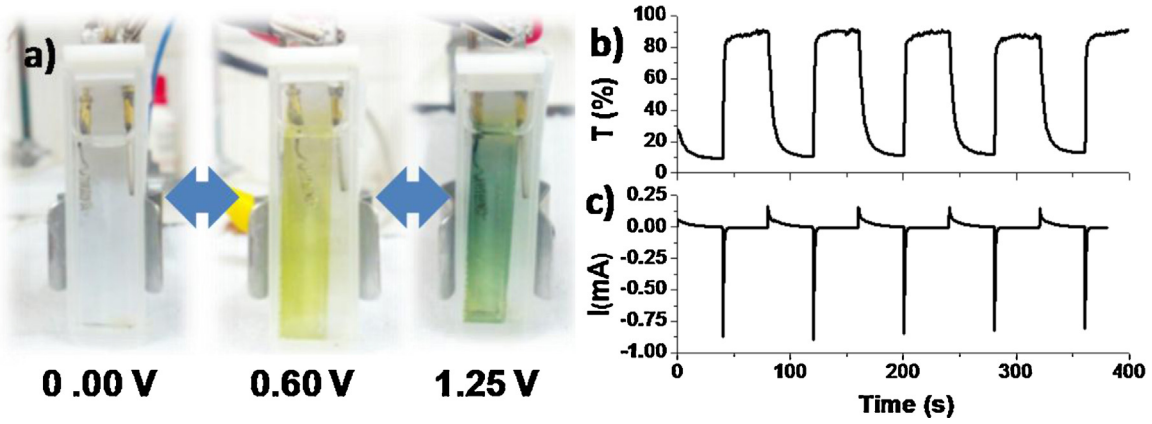

Fig. 9. a) 1 film on an ITO electrode pictures at different applied potentials. b) Dynamic transmittance changes upon switching the potential between 0 and 1.25 V with a pulse width of 40 s applied to the electrodeposited ITO/film of 1 in DCE containing 0.1 M TBAHFP. The absorption was recorded at 772 nm. c) Current generated by the step potentials applied to the system.

observed chances in coloration are less intense than those generated by the alteration of the redox state in film **1** electrodes.

On the other hand, it is known that the film surface morphology characteristics are associated to their use as active layer in electronic and/or optoelectronic devices [21,38] Fig. 10 shows SEM images of both **1** and **3** derivates electropolymer films surfaces, obtained in the above described condition on ITO electrode. Both polymeric films fully cover the ITO surface, but it is clearly seen that they exhibit different morphologies. Besides that both films display granulate surfaces, polymer obtained from **1** has a smaller grain size than the observed for the film produced by the electropolymerization of dendrimer **3**. The morphology differences could be originated in the dendrimeric molecular characteristics. In the case of dendrimer **3**, the relevant fact is the presence of the TPA electroactive central core, which remains positively charged during the electrodeposition processes. As it was already demonstrated the presence of an oxidized core can influence the characteristic of the morphological surface of the hyperbranched polymers obtained by electropolymerization [21,22].

4. Conclusion

We developed a versatile synthetic strategy for the construction of fully conjugated dendrimeric structures using a Sonogashira cross coupling protocol as a key reaction. The starburst dendrimers were built convergently with an electroactive TPA core or a non electroactive TEB core. The branched structures undergo electrochemical polymerization through the oxidation of the peripheral CBZ groups. By this methodology hyperbranched polymers were deposited as conductive films over metallic and semitransparent oxide electrodes. The effects of monomer structural characteristics over the films morphological and physiochemical properties were elucidated. In this way, the importance of the presences of an extended conjugation in the dendrimer branches for efficient film formation has been evidenced. We have also shown that the existence of an oxidized core in the dendrimeric structure affects both, the electrochromic and film morphology properties. Thus, the electroactive hyperbranched starburst polymeric films, with the capability to avoid staking or aggregation between the redox centers, have a remarkable potential to find applications in the design and construction of organic electro-optical devices.

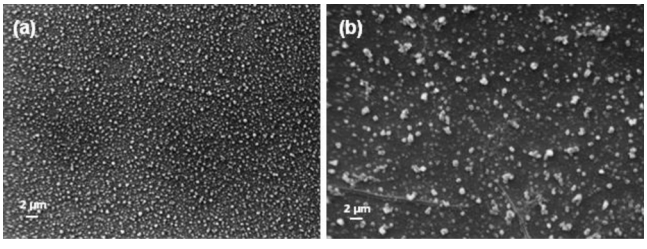

Fig. 10. SEM photographs of dendrimeric electropolymer films surfaces obtained from a) 1 and b) 3.

ACKNOWLEDGMENTS

We thank Consejo Nacional de Investigaiones Cientificas y Tecnicas (CONICET-Argentina), Agencia Nacional de Promoción Cientıfica y Tecnológica (ANPCYT Argentina), Universidad Nacional de Rosario y Universidad Nacional de Río Cuarto. M.I.M, R.A.S, D.H, L.F, L.O. and F.F. are scientific members of CONICET.

Appendix A. Supplementary data

Supplementary data associated with this article can be found, in the online version, at http://dx.doi.org/10.1016/j.electacta.2016.04.154.

References

[1] J.J. Frechet, D.A. Tomalia, Dendrimers and Other Dendrimetic Polymers, Wiley Series in Polymers Science, John Wiley & Sons Ltd., 2001.
[2] T. Sudyoadsuk, V. Promarak, R. Rattanawan, T. Keawin, S. Jungsuttiwong, T. Sudyoadsuk, V. Promarak, Carbazole dendronised triphenylamines as solution processed high Tg amorphous hole-transporting materials for organic electroluminescent devices, Chem. Commun. 48 (2012) 3382.
[3] K. Albrecht, R. Pernites, M.J. Felipe, R.C. Advincula, K. Yamamoto, Patterning carbazole-phenilazomethine dendrimer films, Macromolecules 45 (2012) 1288.
[4] J.L. Wang, Y. Zhou, Y. Li, J. Pei, Solution-Processable Gradient Red-Emitting π-Conjugated Dendrimers Based on Benzothiadiazole as Core: Synthesis Characterization and Device Performances, J. Org. Chem. 74 (2009) 7449.
[5] T. Qin, W. Wiedemair, S. Nau, R. Trattnig, S. Sax, S. Winkler, A. Vollmer, N. Koch, M. Baumgarten, E.J.W. List, K.J. Müllen, Core Shell and surface-optimized dendrimers for blue ligth-emitting diodes, J. Am. Chem. Soc. 133 (2011) 1301.
[6] R.M. Adhikari, R. Mondal, B.K. Shah, D.C. Neckers, Synthesis and photophysical properties of carbazole-based blue light-emitting dendrimers, J. Org. Chem. 72 (2007) 4727.
[7] T.W. Kwon, M.M. Alam, S.A. Jenekhe, n-type conjugated dendrimers: Convergent synthesis, photophysics, electroluminiscence, and use as electron-transport materials for light-emitting diodes, Chem. Mater. 16 (2004) 4657.
[8] P.L. Burn, S.C. Lo, I.D. Samuel, Effect of generation and soft lithography on semiconducting dendrimer lasers, Adv. Mater. 19 (2007) 1675.
[9] S.C. Lo, P.L. Burn, Development of dendrimers: Macromolecules for use in organic light-emitting diodes and solar cells, Chem. Rev. 107 (2007) 1097.
[10] T. Nakashima, N. Satoh, K. Albrecht, K. Yamamoto, Interface modification on TiO_2 electrode using dendrimers in dye-sensitized solar cells, Chem. Mater. 20 (2008) 2538.

[11] J. Lu, P.F. Xia, P. Lo, Y. Tao, M.S. Wong, Synthesis and properties of multi-triarylamme-substituted carbazole-based dendrimers with an oligothiophene core for potential applications in organic solar cells and light-emitting diodes, Chem. Mater. 18 (2006) 6194.
[12] P. Rajakumar, A. Thirunarayanan, S. Raja, S. Ganesan, P. Maruthamuthu, Photophysical properties and dye-sensitized solar cell studies on thiadiazole-triazole-chalcone dendrimers, Tetrahedron Lett. 53 (2012) 1139.
[13] K.A. Alamry, N.I. Georgiev, S.A. El-Daly, L.A. Taib, V.B. Bojinov, A highly selective ratiometric fluorescent pH probe based on a PAMAM wavelength-shifting bichromophotic system, Spectrochim. Acta A 135 (2015) 792.
[14] G. Singh, V. Bhalla, M. Kumar, Carbazole end-capped and triphenylamine-centered starburst derivative for hole-transport in electroluminescent devices, Opt. Mater. 46 (2015) 82.
[15] S. Orlandi, G. Pozzi, M. Cavazzini, D. Minudri, M. Gervaldo, L. Otero, F. Fungo, Synthesis and properties of an electropolymer obtaines from a dimeric donor/acceptor system with a 4,4′-spirobi[cyclopenta[2,1-b:3,4-b']dithiophene]core, Macromolecules 48 (2015) 4364.
[16] L. Otero, L. Sereno, F. Fungo, Y.L. Liao, C.Y. Lin, K.T. Wong, Synthesis and Properties of a Novel Electrochromic Polymer Obtained from Electropolymerization of 9,9′-Spirobifluorene-bridged Donor-Acceptor (D-A) Bichromophore System, Chem. Mat. 18 (2006) 3495.
[17] J. Natera, L. Otero, L. Sereno, F. Fungo, N.S. Wang, Y.M. Tsai, T.Y. Hwu, T.K. Wong, A Novel Electrochromic Polymer Synthesized through Electropolymerization of a New Donor-Acceptor Bipolar System, Macromolecules 40 (2007) 4456.
[18] K.T. Wong, L. Yu-Hsien, H.H. Wu, F. Fungo, Synthesis and properties of dumbbell-shaped dendrimers containing 9-phenylcarbazole dendrons, Org. Lett. 9 (2007) 4531.
[19] P. Zabel, T. Dittrich, Y.I. Liao, C.Y. Lin, K.T. Wong, L. Fernández, F. Fungo, L. Otero, Engineering of a gold surface work function by electrodeposition of a spiro compound with a donor-acceptor pair, Organic Electronics 10 (2009) 1307.
[20] J. Natera, N.S. Wang, Y.M. Tsai, K.T. Wong, L. Otero, F. D'Eramo, L. Sereno, F. Fungo, Synthesis and Properties of a Novel Cross-linked Electroactive Polymer from a Bipolar Starburst Monomer, Macromolecules 42 (2009) 626.
[21] D. Heredia, L. Fernandez, L. Otero, M. Ichikawa, C.Y. Lin, Y.L. Liao, S.A. Wang, K.T. Wong, F. Fungo, Electrochemical tuning of morphological and optoelectronic characteristics of donor-acceptor spiro-fluorene polymer film. Application in the building of an electroluminescent device, J. Phys. Chem. C 115 (2011) 21907.
[22] M.I. Mangione, R.A. Spanevello, A. Rumbero, D. Heredia, G. Marzari, L. Fernandez, L. Otero, F. Fungo, Macromolecules 46 (2013) 4754–4763.
[23] S.M. Grayson, J.M. Fréchet, Convergent dendrons and dendrimers: from synthesis to applications, Chem. Rev. 101 (2001) 3819.
[24] C.J. Hawker, K.L. Wooley, The convergence of synthetic organic and polymer chemistries, Science 309 309 (2005) 1200.
[25] D.A. Tomalia, Starburst™/cascade dendrimers: fundamental buildingblocks for a new nanoscopic chemistry set, Aldrichimica Acta 26 (1993) 91.
[26] H. Nonami, S. Fukui, R.J. Erra-Balsells, β-Carboline alkaloids as matrices for matrix-assisted ultraviolet laser desorption time-of-flight mass spectrometry or proteins and sulfated aligosaccharides: a comparative study using phenylcarbonyl compounds, carbazoles and classical matrices, Mass Spectrom. 32 (1997) 287.
[27] C.M. Cardona, W. Li, A.E. Kaifer, D. Stockdale, G.C. Bazan, Electrochemical considerations for determining absolute frontier orbital energy levels of conjugated polymers for solar cell applications, Adv. Mater. 23 (2011) 2367.
[28] G.E. Johnson, A Spectroscopic Study of Carbazole by Photoselection, J. Phys. Chem. 78 (1974) 1512.
[29] H. Ohkita, S. Ito, M. Yamamoto, Y. Tohda, K. Tani, Intramolecular excimer emissions of syn- and anti-[3.3](3,9)carbazolophanes in solutions, J. Phys. Chem. A 106 (2002) 2140.
[30] Y.J. Cho, K.R. Wee, H.J. Son, D.W. Cho, S.O. Kang, A detailed investigation of light-harvesting efficiency of blue color emitting divergent iridium dendrimers with peripheral phenylcarbazole units, Phys. Chem. Chem. Phys. 16 (2014) 4510.
[31] K. Ray, T.N. Misra, Spectroscopic Study of Nonamphiphilic 9-Phenylcarbazole Assembled in Langmuir-Blodgett Films, Langmuir 13 (1997) 6731.
[32] R.M. Adhikari, R. Mondal, B.K. Shah, D.C. Neckers, Synthesis and Photophysical Properties of Carbazole-Based Blue Light-Emitting Dendrimers, J. Org. Chem. 72 (2007) 4727.
[33] S.I. Kato, H. Noguchi, A. Kobayashi, T. Yoshihara, S. Tobita, Y. Nakamura, Bicarbazoles: systematic structure-property investigations on a series of conjugated carbazole dimers, J. Org. Chem. 77 (2012) 9120.
[34] J.C. Sciano, Handbook of Organic Photochemistry, vol. 1, CRC Press, Boca Raton, FL, 1989, pp. 231.
[35] S. Lu, T. Liu, L. Ke, D.G. Ma, S.J. Chua, W. Huang, Polyfluorene-Based Light-Emitting Rod Coil Block Copolymers, Macromolecules 38 (2005) 8494.
[36] S.K. Chiu, Y.C. Chung, G.S. Lioua, Y.O. Su, Electrochemical and Spectral Characterizations of 9-Phenylcarbazoles, J. Chin. Chem. Soc. 59 (2012) 331.
[37] O. Yurchenko, D. Freytag, L. Zur Borg, R. Zentel, J. Heinze, S. Ludwigs, Electrochemically Induced Reversible and Irreversible Coupling of Triarylamines, J. Phys. Chem. B 116 (2012) 30.
[38] M. Li, S. Tang, F. Shen, M. Liu, W. Xie, H. Xia, L. Liu, L. Tian, Z. Xie, P. Lu, M. Hanif, D. Lu, G. Cheng, Y. Ma, Electrochemically deposited organic luminescent films: the effects of deposition parameters on morphologies and luminescent efficiency of films, J. Phys. Chem. B 110 (2006) 17784.